Available online at www.sciencedirect.com
ScienceDirect
Journal of the European Ceramic Society 28 (2008) 1297–1303
www.elsevier.com/locate/jeurceramsoc

Processing of carbide-derived carbon (CDC) using biomorphic porous titanium carbide ceramics

Martina Kormann, Hanadi Ghanem, Helmut Gerhard, Nadejda Popovska *

Department of Chemical Reaction Engineering, University of Erlangen-Nuremberg, Egerlandstrasse 3, D-91058 Erlangen, Germany

Received 19 April 2007; received in revised form 11 July 2007; accepted 20 July 2007
Available online 23 October 2007

Abstract

Biomorphic porous TiC and TiC/TiO_2 ceramics were covered with highly porous carbon, so-called carbide-derived carbon (CDC), by selective etching of Ti from TiC with chlorine containing gas in a temperature range 400–1000 °C. The etching rate of TiC is strongly affected by the chlorine concentration, but only slightly by the reaction temperature. No correlation was found between etching rate of TiC and specific surface area (SSA) of the resulting CDC with respect to temperature. Kinetic investigations show that for up to 80 min the etching process is controlled by the chemical reaction. At longer times a diffusion limitation has to be taken into account. Addition of hydrogen to the etching gas enhances the diffusion of the chlorine molecules, so that no diffusion limitation was observed. Microporous carbon with narrow pore size distribution was obtained at temperatures ranging from 400 to 800 °C. Treatment at higher temperatures leads to formation of mesopores. The CDC produced by chlorination of TiC at 400 °C is amorphous. Increased reaction temperature and addition of hydrogen to the chlorine gas lead to formation of regions with higher order like onion carbon and graphitic ribbons. The CDC coated TiC/TiO_2 ceramics with predominantly anatase phase show enhanced photo catalytic activity.

Keywords: Carbide-derived carbon; Films; Diffusion; TiC; Porosity

1. Introduction

Porous solids are of great technological importance due to their ability to interact with solids and liquids not only on the surface, but also through their bulk. Although large pores can be produced and well controlled in a variety of materials, nanoporous carbon because of its high specific surface area with a tuneable, very narrow, pore size distribution, has received much attention recently due to many potential applications as adsorbents, catalyst supports, electrodes and hydrogen storage systems. Carbide-derived carbon (CDC) represents a new class of these nanoporous carbons, produced by selective thermochemical etching of inorganic carbon containing materials such as metal carbides. The structure of the CDC can be templated by the initial carbide structure, with the opportunity for further structural modifications by controlling the process parameters like temperature, total pressure, etching agent type and concentration.

Review of the literature data on CDC shows that the etching process is possible using a variety of carbides like B_4C,[1] Ti_2AlC,[2] TiC,[3] SiC,[4] Ti_3SiC_2.[5] Among them is SiC the most investigated template for this process.

Titanium carbide (TiC) is also a very promising candidate for producing CDC. TiC as starting material shows a small and uniform carbon–carbon distance and this may lead to a highly porous carbon with narrow pore size distribution.[6] These results on CDC from TiC show that amorphous carbon is produced and that the specific surface area increases with etching temperature in a temperature range from 400 to 1000 °C. After 3 h treatment in chlorine atmosphere a specific surface area of 1200 m^2/g up to 1800 m^2/g is reached at 400 and 800 °C, respectively. At higher temperatures a graphitisation of carbon results in a small decline in SSA. In general, etching temperatures below 1000 °C result in amorphous carbon whereas temperatures above 1000 °C lead to graphitisation of the carbon resulting in a decrease of the SSA. Purging with H_2 at 600 °C increases SSA because of the

* Corresponding author.
E-mail address: n.popovska@rzmail.uni-erlangen.de (N. Popovska).

0955-2219/$ – see front matter © 2007 Elsevier Ltd. All rights reserved.
doi:10.1016/j.jeurceramsoc.2007.07.018

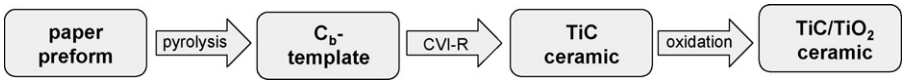

Fig. 1. Overall scheme for production of porous TiC and TiC/TiO_2 ceramics.

removal of residual chlorine from the pores. Investigations on chlorination on TiC powder revealed onion-like structure of the produced carbon at a chlorination time for 1 h at 900 °C. These structures with concentric spherical graphitic shells were observed to have outer diameters in the range of 15–35 nm. The distance between graphitic planes in the shells was 0.34 nm, slightly larger than the interplanar distance in graphite.[7] Further investigations on pore size and pore size distribution were made which show that micro pores (<2 nm) are formed in a temperature range of 400–700 °C.[3,7] With increasing chlorination temperature the average pore size is increased and for reaction temperatures higher than 1000 °C the pore size distribution is broadened and mesopores are detected.[3] The effect of metals, such as iron, nickel and cobalt on the treatment of TiC in chlorine gas was studied in Ref.[8] It was shown, that catalytically active metals support the formation of better-organised carbon structures like graphitic lamellas.

Most investigations on the field of CDC are based on metal carbides in the form of powder. The reaction kinetics and conditions for diffusion limitations have been little studied. Furthermore, almost no information is published about the influence of temperature, etching agent and time on the etching rate.

In this work, porous carbons were prepared by CDC approach according to reactions (1) and (2) using porous TiC and TiC/TiO_2 structures produced from paper preforms by chemical vapor infiltration and reaction (CVI-R) technique.[9]

$$TiC + 2Cl_2 \rightarrow TiCl_4 + C \quad (1)$$

$$TiC + 3Cl_2 + H_2 \rightarrow TiCl_4 + C + 2HCl \quad (2)$$

It is important to point out that the formation of carbon on the surface is uniform and does not change the shape of the initial TiC and TiC/TiO_2 ceramics allowing preparation of structures with complex geometry and high mechanical stability. The idea is to use these structures as adsorbent, catalyst or catalyst support because of their easier separation from the reaction mixture. CDC coated TiC/TiO_2 porous ceramic is expected to show enhanced photo catalytic activity because of high specific surface area.[10]

2. Experimental work

2.1. Processing of biomorphic porous ceramics by CVI-R technique

Biomorphic porous TiC and TiC/TiO_2 ceramics derived from paper preforms were produced by chemical vapor infiltration and reaction technique in a three-step process according to the following scheme (Fig. 1). Details are given in Refs.[9,11] The paper preform (3 cm × 3 cm) consisting mainly of cellulose fibres was converted into carbon biotemplate (C_b) by pyrolysis in inert atmosphere, followed by chemical vapor infiltration at 1100 °C and atmospheric pressure with $TiCl_4/CH_4/H_2$ as precursor system according to the following equation[11]:

$$(x+y)TiCl_4 + xCH_4 + yC_b \rightarrow xTiC + yTiC_b + 4(x+y)HCl \quad (3)$$

The last processing step was oxidation of TiC in order to produce TiC/TiO_2 ceramics. The oxidation was conducted in air flow for 20 h at 400 °C.

2.2. Processing of carbide-derived carbon (CDC) by selective etching of TiC ceramic

The porous TiC ceramic was covered with a carbon layer by selective etching in chlorine or chlorine/hydrogen gas mixtures at temperatures in the range 400–1000 °C at atmospheric pressure (Fig. 2). The gas mixtures consist of helium with 0.020 or 0.026 mol/h Cl_2 without or with addition of H_2 ($Cl_2/H_2 = 4$). The chlorination times vary between 20 min and 4 h.

The TiC/TiO_2 mixed ceramic was treated with chlorine/hydrogen gas mixture for a short time of 10 min at low temperature of 400 °C in order to obtain thin carbon layer retaining the catalytic active anatase modification of TiO_2 (Fig. 2).

The TiC samples were placed in the isothermal zone of a horizontal hot-wall tubular flow reactor operated at atmospheric pressure and heated up to the reaction temperature by 5 °C/min under a helium flow. Once the desired temperature was reached, chlorine or chlorine/hydrogen gas mixture with a gas velocity of 1.5 cm/s was passed through the alumina tube with 3.2 cm inner diameter and a heated length of 100 cm. After chlorination, the furnace was cooled down to room temperature in helium atmosphere. The etching rate was calculated as mass loss (mg)/unit time (h).

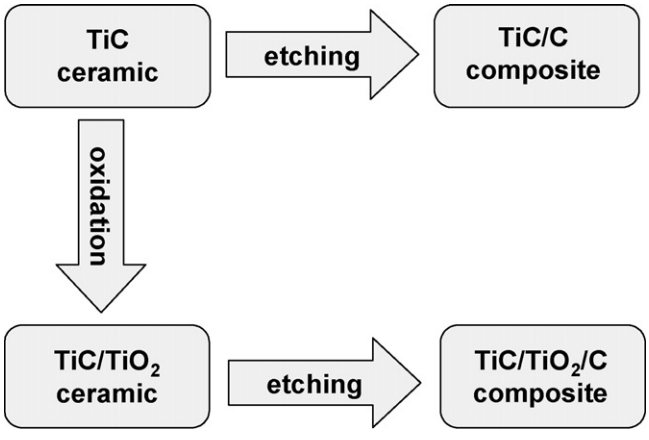

Fig. 2. Processing scheme for CDC coated TiC and TiC/TiO_2 ceramics.

2.3. Characterisation methods

The resulting carbon–ceramic composites (CDC-TiC and CDC-TiC/TiO_2) were characterised by Raman spectroscopy. Raman spectra from 100 to 2000 cm^{-1} were collected using Raman spectrometer equipped with an Ar^+ laser ($\lambda = 633$ nm) at 50× magnification in order to investigate the structure of the carbon formed.

Gas sorption analysis was performed using a Gemini 2370 from Micromeritics GmbH with nitrogen as adsorbates at −195.8 °C. It was used to calculate the specific surface area (SSA) and the pore volume. The porosity of the ceramics was determined by Hg-porosimetry with Carlo Erba Mercury Intrusion Porosimeter 2000.

Coaxial double ring bending tests (INSTRON Model 4204) were carried out to measure the bending strength of the ceramic samples according to German Standard Code DIN 52,292.

The morphology of the samples was investigated by scanning electron microscopy coupled with energy dispersive X-ray analysis (SEM/EDX, JSM-6400) to determine the composition of the surface layer.

Thermodynamic calculations were performed with Gibbs energy minimization software HSC Chemistry®. This is thermochemical software designed for the calculation of various kinds of chemical reactions and thermodynamic equilibria to make conventional thermodynamic calculations fast and easy to carry out.

3. Results and discussion

3.1. Parameter screening of the etching process of TiC ceramic

3.1.1. Kinetics of the chlorination of TiC

The kinetics of the chlorination process was investigated at 400 °C and presented in Fig. 3 by plotting the etched mass as a function of reaction time for chlorine and chlorine/hydrogen as etching agent. According to the literature,[6] the CDC layer thickness increased linearly with the reaction time indicating no control by diffusion. Looking at the curves in Fig. 3, it can be seen that it is the case only at etching times in the region up to 80 min, where the amount of etched titanium is nearly linearly increased from 106 mg in 20 min up to 336 mg in 80 min. At longer reaction time the process is limited by diffusion of the reactive gas through the formed carbon layer in order to react with TiC.

Addition of small amount hydrogen to chlorine gas ($Cl_2/H_2 = 4$) results in a 20–25% lower etching rate due to the lower reactivity of the HCl as etching agent. The progression of the kinetic curve looks also different. No clear diffusion limitation seems to occur up to 240 min reaction time. Hydrogen enhances the diffusion of the chlorine molecules as described in the literature[4] and enlarges the specific surface area of the carbon formed. Thus, hydrogen addition can avoid diffusion limitation and it is useful especially at longer etching times to achieve high etching rate and CDC with high SSA.

Thermodynamic calculations show the possibility to etch carbon to CCl_4 by treatment with chlorine at temperatures up to 600 °C.[6] To prove this, experiments were conducted with the initial C_b-template etching it at the same chlorination condition. However, no mass loss could be measured indicating that this reaction is kinetically inhibited.

3.1.2. Effect of temperature and chlorine concentration on the etching rate of TiC and the SSA of the resulting CDC

The etching rate of TiC at different temperatures and chlorine concentrations is presented in Fig. 4. Increasing the temperature up to 600 °C leads to higher etching rates especially at higher chlorine concentration. However, in the range 600–1000 °C almost no temperature dependence of the etching rate could be observed. Thus, the temperature has less effect on the etching process than chlorine concentration.

The effect of the etching conditions on the specific surface area of the resulting CDC is shown in Fig. 5. The curves show similar temperature dependence of the SSA, independent from the chlorine concentration used. In both cases SSA is linearly increased by raising the reaction temperature up to 800 °C, where a maximum value of SSA is achieved. A further increase of the temperature results in CDC with lower SSA due to changes in the microstructure as well as in the pore structure, as shown below. Comparing Figs. 4 and 5 it can be concluded, that there

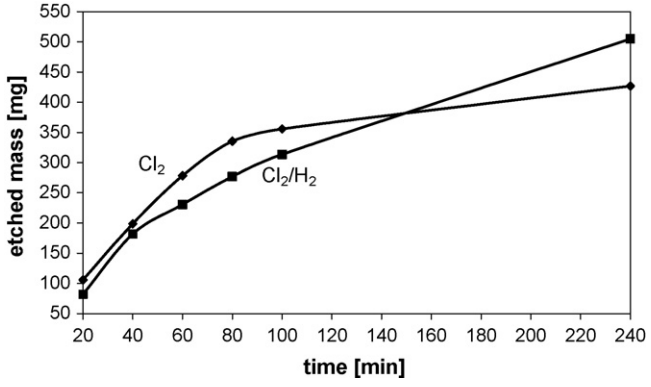

Fig. 3. Kinetic curves of the etching reaction with chlorine and chlorine/hydrogen ($Cl_2/H_2 = 4$) mixture at 400 °C.

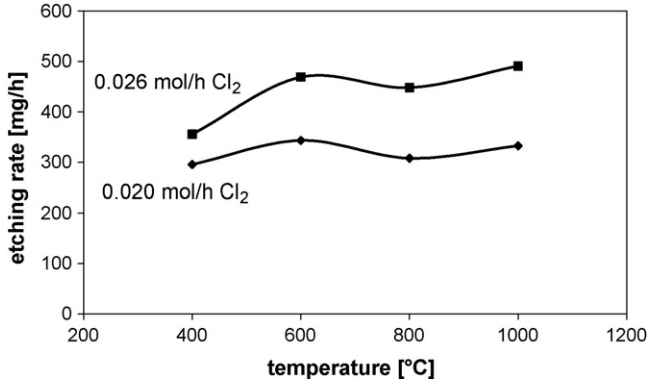

Fig. 4. Etching rate of TiC at different temperatures and chlorine concentrations for 1 h etching time.

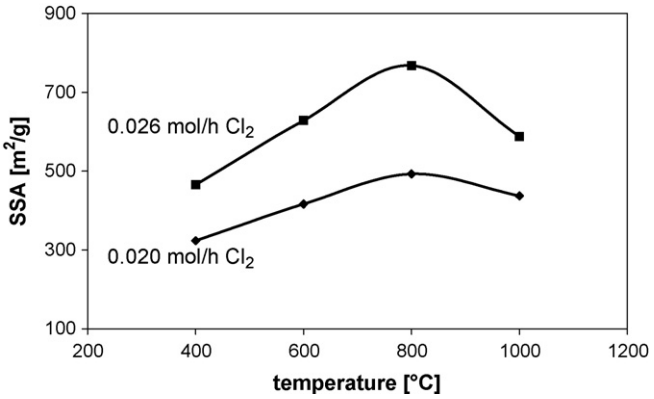

Fig. 5. Specific surface area (SSA) of CDC obtained at different etching conditions for 1 h etching time.

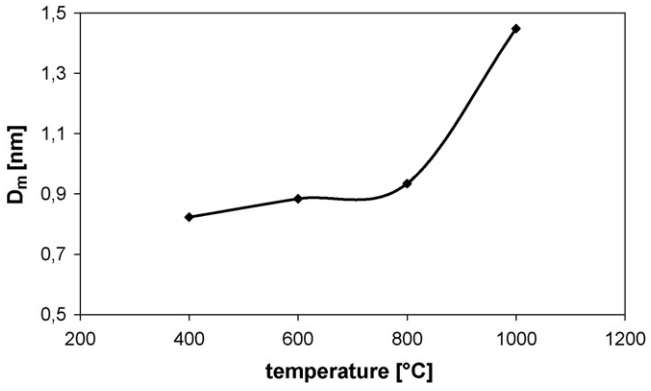

Fig. 7. Mean pore diameter for CDC obtained at different temperatures (Fig. 6).

is no correlation between etching rate of TiC and SSA of the resulting CDC.

3.2. Microstructure of CDC

3.2.1. Pore structure

The pore structure of CDC derived from TiC at different reaction temperature in the range 400–1000 °C was investigated by low temperature nitrogen adsorption. The adsorption isotherms of samples chlorinated at 400, 600 and 800 °C are of type I of the Brunauer classifications,[12] which is consistent with a microporous material with pore size less than 2 nm. The adsorption isotherm at 1000 °C shows a hysteresis and, therefore, is of type IV in the same classification scheme, indicating presence of mesopores. The pore size distribution of the CDC obtained at different temperatures is presented in Fig. 6. The sample etched at low temperature shows narrow distribution (Fig. 6a), whereas broadening of the curves with the temperature is visible (Fig. 6b–d). The mean diameter of the pores (D_m) increases with increasing the chlorination temperature (Fig. 7). The observed differences in the pore size are due to changes in the CDC microstructure on increasing the reaction temperature. It seems that the narrow pore size distribution at 400 °C is associated with amorphous carbon and formation of larger mesopores results in places with graphitic structures. Similar trends were found by chlorination of Ti_2AlC.[2]

3.2.2. Raman spectroscopy

The CDC structure was examined by Raman spectroscopy (Fig. 8). The spectra show the two characteristic peaks for carbon- the D-band at 1330–1342 cm^{-1} and G-band at 1585–1600 cm^{-1}. A much higher intensity of disordered-induced D-band compared with G-band, corresponding to in plane vibration of carbon atoms in graphite, suggests in all cases a nanocrystalline and disordered structure of CDC. However,

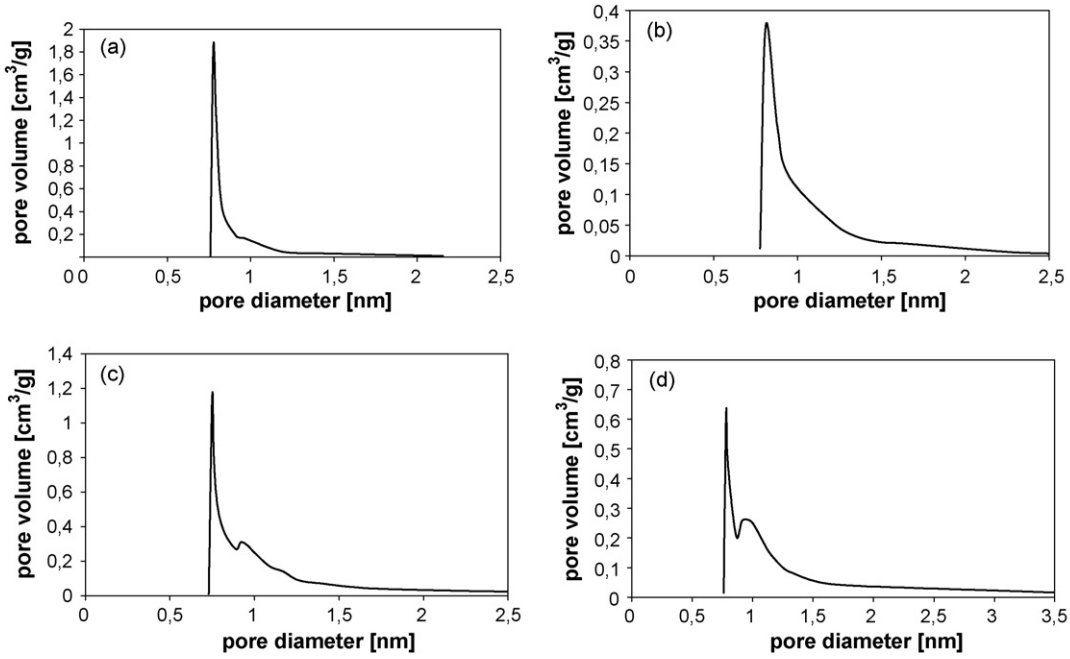

Fig. 6. Horvath-Kawazoe pore size distribution of CDC obtained at different chlorination temperatures, (a) 400 °C, (b) 600 °C, (c) 800 °C and (d) 1000 °C with 0.020 mol/h Cl_2, 1 h.

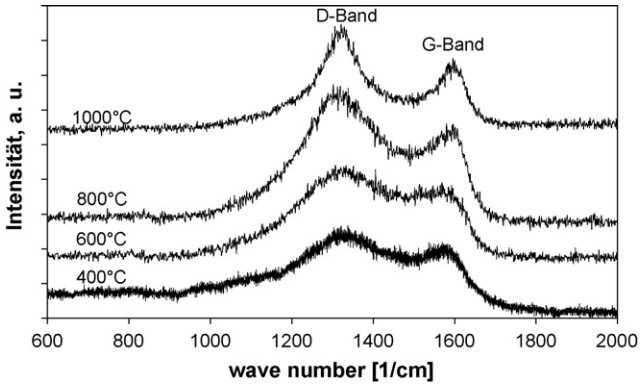

Fig. 8. Raman spectra of samples chlorinated at different temperatures with 0.020 mol/h Cl_2 for 1 h.

increasing the chlorination temperature results in a decrease of full width at half maximum (FWHM) of D- and G-band indicating a substantial increase of ordered carbon in particular above 800 °C.

3.2.3. Morphology of CDC

The surface morphology of TiC-ceramics before and after chlorination at 600 °C was investigated by scanning electron microscopy (SEM) and presented in Fig. 9. A difference in the fibre structure can easily be recognized. Whereas the TiC fibres look quite irregular in size and thickness, the CDC-TiC fibres seem to be bloated because of the porous structure. The element composition of the layer was estimated by EDX analysis at the marked positions in the images (Table 1). After chlorination of the TiC samples the Ti content decreases from 41.5 to 2.0 at.% and they consist mainly of carbon. Oxygen and sulphur impurities were detected in small amount as well.

Table 1
EDX analysis of element composition of TiC (position 1) and CDC-TiC (position 2)

at.%	Position 1	Position 2
C	58.5	94.5
O	–	2.7
S	–	0.8
Ti	41.5	2.0

3.2.4. TEM

TEM studies of CDC-TiC reveal their microstructure at atomic scale. Whereas etching with chlorine at 400 °C results in formation of mainly amorphous carbon (Fig. 10a), chlorination at 600 °C with chlorine/hydrogen gas mixture results in formation of more ordered carbon structures (Fig. 10b). The main part consists of amorphous carbon but the addition of hydrogen to the reactive gas favours the formation of onion-like carbon. The TEM micrograph shows also some isolated sites of well-ordered graphitic sheets within amorphous carbon. Literature review confirms the formation of onion-like carbon but it is described for temperatures of about 900 °C in pure chlorine atmosphere.[7] Admixture of hydrogen promotes the creation of better ordered structures such as onion-like carbon. A HRTEM micrograph of a

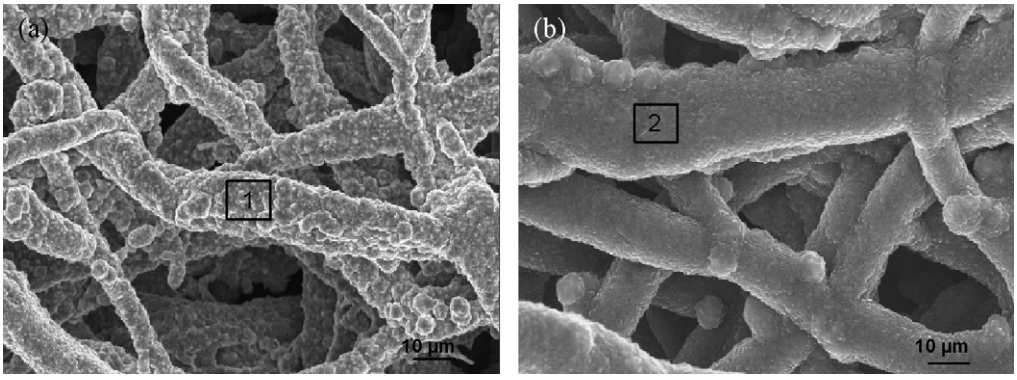

Fig. 9. SEM images of (a) TiC ceramic and (b) CDC-TiC ceramic.

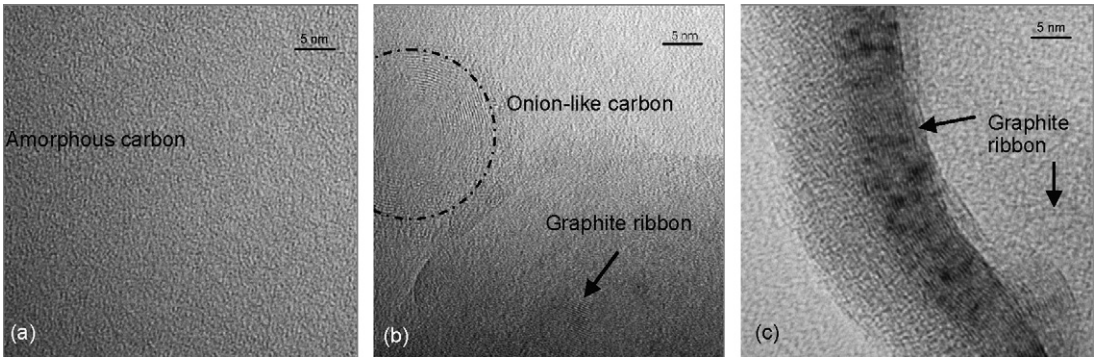

Fig. 10. HRTEM micrographs of CDC-TiC chlorinated for 1 h at (a) 400 °C, (b) 600 °C and (c) 1000 °C.

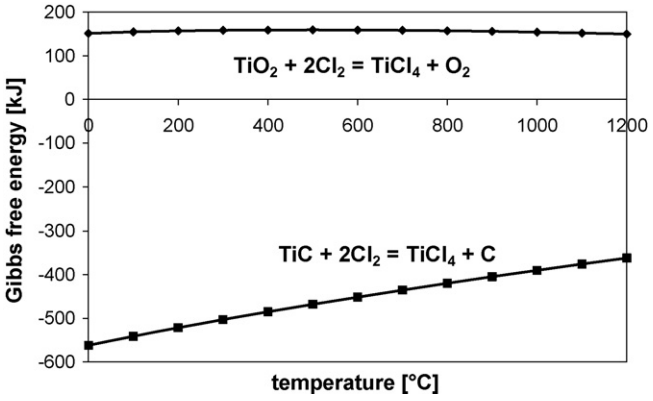

Fig. 11. Thermodynamic stability of TiC and TiO_2 during chlorination process.

sample treated at 1000 °C shows a well-ordered graphitic ribbon within amorphous carbon (Fig. 10c). The ribbon has a thickness of about 5 nm, which corresponds to 15 graphene layers. Curved graphitic structures were not found in this sample and no complete graphitisation is visible. This result agrees well with the results of Raman spectroscopy, where the D-peak is still better pronounced as the G-peak. All analyses suggest a greater grade of order of CDC with increasing reaction temperature.

3.2.5. Mechanical properties of CDC-TiC

The mechanical stability of the CDC-TiC composites was estimated by measuring their bending strength. The initial TiC ceramics show a bending strength of 45–50 MPa at a porosity of 60%. After chlorination for 4 h with the chlorine/hydrogen gas mixture at different temperatures the samples retain their mechanical stability. Both, bending strength and porosity are not affected by the etching temperature. A bending strength of 16–18 MPa at porosity of around 60% is measured even after long etching time, where over 90% of the TiC was converted to carbon. The CDC layer is adherent and the composites show high shape as well as mechanical stability.

3.3. Processing of carbon coated TiO_2 by selective etching of TiC/TiO_2 ceramics

The CDC approach was also applied on the TiC/TiO_2 ceramics in order to produce carbon layers with high specific surface area. It is expected, that carbon coated TiO_2 will show enhanced photo catalytic activity as reported in the literature.[13] However, it has to be proved by thermodynamic calculations whether the Ti from TiO_2 will also be etched by chlorination, which would be unfavourable because of the destruction of the photo catalyst.

The thermodynamic calculations with the HSC software have shown (Fig. 11) that the reaction of chlorine with TiO_2 is thermodynamically not favourable. Therefore, it is possible to apply the CDC-method on the mixed ceramics without destroying the photo catalytic active TiO_2 layer.

In previous work[9] the processing of biomorphic TiC/TiO_2 ceramics was studied in detail. It was found, that the oxidation temperature of TiC affects the anatase/rutile ratio of the resulting TiO_2 samples. The catalytically more active anatase phase is formed at temperatures below 600 °C. Therefore, the TiC/TiO_2 ceramics produced by oxidation of biomorphic TiC at 400 °C in air flow[9] were etched for 10 min at 400 °C in Cl_2/H_2 mixture to produce a thin carbon layer on the TiO_2 surface. The amount of carbon is calculated to be 1.8 wt%. As a result, the specific surface area of the resulting ceramic composite was increased significantly as shown in Table 2. The CDC coated TiC/TiO_2 ceramics show enhanced photo catalytic activity by degradation of 4-chlorophenol (4-CP) under UV light due to the improved adsorption capacity. The results will be presented in a separate paper.

Table 2
Specific surface area (SSA) of biomorphic ceramics

Sample	TiC	TiC/TiO_2	CDC-TiC/TiO_2
SSA (m^2/g)	0.7	17.7	63.4

4. Conclusions

Biomorphic porous TiC and TiC/TiO_2 ceramics produced from paper preforms by chemical vapor infiltration and reaction technique can be covered with highly porous carbon by selective etching of Ti from TiC with chlorine containing gas in a temperature range 400–1000 °C. Calculations of the Gibbs free energy have shown that at these conditions the reaction of Ti from TiO_2 with chlorine is thermodynamically not favourable.

The etching rate of TiC is affected by the chlorine concentration, but only slightly by the reaction temperature. Kinetic investigations have shown that for up to 80 min the etching process is controlled by the chemical reaction. At longer treatment times diffusion limitation has to be taken into account. Addition of hydrogen to the etching gas enhances the diffusion of the chlorine molecules, so that no diffusion limitation was observed. Thus, hydrogen addition can avoid diffusion limitation and it is useful especially at longer etching times to achieve high etching rate and CDC with high SSA.

The pore structure of CDC can be tuned by the etching temperature. Microporous carbon with narrow pore size distribution was obtained at temperatures ranging from 400 to 800 °C. Treatment at higher temperatures leads to formation of mesopores. No correlation was found between etching rate of TiC and specific surface area of the resulting CDC.

The CDC produced by chlorination of TiC at 400 °C is amorphous. Increased reaction temperature and addition of hydrogen to the chlorine gas lead to formation of higher ordered regions like onion carbon and graphitic ribbons as shown by Raman spectroscopy and TEM.

The CDC coated TiC/TiO_2 ceramics with predominantly anatase phase show enhanced photo catalytic activity due to the high SSA of 64 m^2/g.

The produced carbon–ceramic composites are mechanically stable and show a bending strength of 16–18 MPa at a porosity of 60%. These structures can be used as adsorbent, catalyst or catalyst support because of their easier separation from the reaction mixture.

References

1. Dash, R. K., Nikitin, A. and Gogotsi, Y., Microporous carbon derived from boron carbide. *Micropor. Mesopor. Mater.*, 2004, **72**, 203–208.
2. Hoffmann, E. N., Yushin, G., Barsoum, M. W. and Gogotsi, Y., Synthesis of carbide-derived carbon by chlorination of Ti_2AlC. *Chem. Mater.*, 2005, **17**, 2317–2322.
3. Dash, R. *et al.*, Titanium carbide derived nanoporous carbon for energy-related applications. *Carbon*, 2006, **44**, 2489–2497.
4. Cambaz, Z. G., Yushin, G. N. and Gogotsi, Y., Formation of carbide-derived carbon on β-silicon carbide whiskers. *J. Am. Ceram. Soc.*, 2006, **89**(2), 509–514.
5. Yushin, G. N., Hoffmann, E. N., Nikitin, A., Ye, H., Barsoum, M. W. and Gogotsi, Y., Synthesis of nanoporous carbide-derived carbon by chlorination of titanium silicon carbide. *Carbon*, 2005, **43**, 2075–2082.
6. Yushin, G., Nikitin, A. and Gogotsi, Y., Carbide derived carbon. In *Handbook of Nanomaterials*, ed. Y. Gogotsi. CRC Press, 2005, pp. 239–282.
7. Zheng, J., Eckström, T. C., Gordeev, S. K. and Jacob, M., Carbon with an onion-like structure obtained by chlorination titanium carbide. *J. Mater. Chem.*, 2000, **10**, 1039–1041.
8. Leis, J., Perkson, A., Arulepp, M., Nigu, P. and Svensson, G., Catalytic effects of metals of the iron subgroup on the chlorination of titanium carbide to form nanostructural carbon. *Carbon*, 2002, **40**, 1559–1564.
9. Ghanem, H., Kormann, M., Gerhard, H. and Popovska, N., Processing of biomorphic porous TiO_2-ceramics by chemical vapor infiltration and reaction (CVI-R) technique. *J. Eur. Ceram. Soc.*, 2007, **27**(12), 3433–3438.
10. Tryba, B., Morawski, A. W., Tsumura, T., Toyoda, M. and Inagaki, M., Hybridization of adsorptivity with photocatalytic activity—carbon-coated anatase. *J. Photochem. Photobiol. A: Chem.*, 2004, **167**, 127–135.
11. Popovska, N., Streitwieser, D. A., Xu, C. and Gerhard, H., Paper derived biomorphic porous titanium carbide and titanium oxide ceramics produced by chemical vapor infiltration and reaction (CVI-R). *J. Eur. Ceram. Soc.*, 2005, **25**(6), 829–836.
12. Webb, P. A. and Orr, C., *Analytical Methods in Fine Particle Technology*. Micromeritics Instrument Corporation, 1997.
13. Lettmann, Ch., Hildenbrand, K., Kisch, H., Macyk, W. and Maier, W. F., Visible light photodegradation of 4-chlorophenol with a coke-containing titanium dioxide photocatalyst. *Appl. Cat. B: Environ.*, 2001, **32**, 215–227.